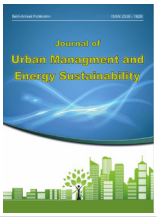
International Journal of Urban Management and Energy Sustainability (IJUMES)

Homepage: http://www.ijumes.com



ORIGINAL RESEARCH PAPER

Technical and Hydrogeological Feasibility Assessment of Environmentally Sustainable Subsurface Dams Using Numerical Modeling: A Case Study of the Rafsanjan Plain Aquifer

Saeid Riahi Riseh, Amir Robati*, Mohammadali Kazerooni Sadi

Department of Civil Engineering, Ke.C., Islamic Azad University, Kerman, Iran

ARTICLE INFO

Article History:
Received 2026-07-12
Revised 2026-10-05
Accepted 2026-10-22

Keywords:
Feasibility assessment; groundwater numerical modeling; MODFLOW; Rafsanjan Plain aquifer; subsurface dam

ABSTRACT

Declining surface-water resources, falling groundwater levels and increasingly severe droughts have intensified the need for low-cost and sustainable water-storage methods in arid regions. Subsurface dams store water within alluvial deposits with negligible evaporation, but their feasibility in large, over-exploited aquifers has rarely been tested with calibrated numerical models. This study assessed the technical and hydrogeological feasibility of environmentally sustainable subsurface dams in the Rafsanjan Plain aquifer, Iran. The study is applied in purpose and descriptive-analytical in method and draws on geological, geotechnical, hydrological and hydrogeological data. Nine criteria, weighted with the Analytic Hierarchy Process, were used to screen the alluvial margins of the plain for candidate sites. A transient MODFLOW model, calibrated and validated against observed groundwater levels, then simulated cut-off walls at the highest-ranked sites with the Horizontal Flow Barrier package under five design and climate scenarios. The model reproduced observed heads with an RMSE of 2.84 m and an MAE of 2.17 m. Suitable sites were confined to the coarse alluvial fans of the southern and southeastern margins. At the preferred site, the barrier raised upstream heads by up to 6.8 m and added 0.52 million m3 of recoverable storage, while reducing downstream subsurface outflow by 27%. Depth to bedrock, alluvial thickness, permeability and effective porosity were decisive for performance and stability. The Rafsanjan Plain aquifer therefore has considerable but spatially limited potential for subsurface dams, which can reduce drought impacts and evaporation losses and improve local water security when combined with groundwater-demand management.

DOI: 10.22034/ijumes.2026.2108047.1418

Running Title: Environmentally Sustainable Subsurface Dams Using Numerical Modeling

NUMBER OF REFERENCES 33

NUMBER OF FIGURES 03

NUMBER OF TABLES 10

*Corresponding Author:
Email: *Ammirrr@yahoo.com*
Phone: 00983433210043
ORCID: https://orcid.org/0000-0001-5086-5932

INTRODUCTION

Groundwater supplies a large share of the water used for irrigation worldwide, and in many dry regions abstraction now exceeds natural replenishment by a wide margin (Famiglietti, 2014; Konikow & Kendy, 2005). Global assessments indicate that depletion has accelerated since the second half of the twentieth century and that the groundwater footprint of several major aquifers is many times larger than their area (Gleeson et al., 2012; Wada et al., 2010). The consequences are not only hydrological: falling water tables raise pumping costs, degrade water quality, cause irreversible aquifer compaction and undermine rural livelihoods that depend on irrigated agriculture. Managing this decline requires measures that reduce demand and, where hydrogeological conditions allow, increase the volume of water that can be stored and recovered locally (Gorelick & Zheng, 2015). Iran is one of the clearest examples of this challenge. Analyses of national monitoring networks and satellite gravimetry show widespread, mostly human-driven groundwater depletion over recent decades, with the steepest declines in the central and eastern arid basins (Ashraf et al., 2021; Joodaki et al., 2014; Noori et al., 2021). The expansion of irrigated agriculture and the weak enforcement of abstraction limits have been identified as key drivers of this crisis (Madani, 2014). A direct and visible outcome is land subsidence, which has been documented by interferometric synthetic aperture radar (InSAR) in many Iranian plains (Motagh et al., 2008). The Rafsanjan Plain in Kerman Province is among the most severely affected aquifers: irrigation of pistachio orchards accounts for most groundwater withdrawals, the aquifer has been in deficit for decades, and subsidence rates exceed several centimetres per year over large areas (Bockstiegel et al., 2024; Motagh et al., 2017). Groundwater quality also deteriorates towards the northwest, where fine-grained sediments and evaporite-bearing formations increase salinity (Hosseininia & Hassanzadeh, 2023). In such regions, conventional water-storage methods, particularly surface dams, face serious limitations. Open reservoirs lose a large part of their storage to evaporation, accumulate sediment, require large areas of land and involve high construction costs and environmental impacts. Subsurface (groundwater) dams offer a complementary or alternative approach. A subsurface dam is a structure that interrupts or reduces the natural flow of groundwater through alluvial deposits and thereby stores water in the pore spaces between soil particles and sediments (Hanson & Nilsson, 1986; Nilsson, 1988). Compared with surface dams, subsurface dams reduce evaporation losses, lower the risk of contamination, need little land acquisition, have fewer adverse environmental impacts and can be built close to the point of use (Ishida et al., 2011; Nilsson, 1988). The most extensive engineering experience comes from the Ryukyu Islands of Japan, where cut-off walls built with the soil-mixed-wall method have created reservoirs with gross capacities of up to about 10 million m3 that are operated much like surface reservoirs (Imaizumi, 2024). Within the broader family of managed aquifer recharge techniques, subsurface dams are among the few that increase storage without requiring an external source of water (Dillon et al., 2019).

The success of a subsurface dam depends strongly on correct site selection and on an accurate understanding of geological and hydrogeological conditions, including alluvial thickness and composition, the presence of an impermeable layer at the base and abutments, the permeability and porosity of the alluvium, and aquifer recharge and discharge conditions (Hanson & Nilsson, 1986; Nilsson, 1988). Neglecting these factors can reduce performance and may render a project technically and economically unjustifiable (Ishida et al., 2011; Nilsson, 1988). Site-selection studies have therefore combined geographic information systems (GIS) with multi-criteria decision analysis (Malczewski, 2006), for example in Mali (Forzieri et al., 2008), northern Pakistan (I. A. Jamali et al., 2014) and arid Iranian watersheds (A. A. Jamali et al., 2018). These studies show

where conditions appear favourable, but a purely descriptive or field-based assessment is insufficient for a final decision, because the behaviour of an aquifer after dam construction depends on complex interactions between groundwater flow, recharge, abstraction and the hydraulic properties of the porous medium. Numerical groundwater modeling can resolve this limitation. MODFLOW, developed by the U.S. Geological Survey, is the most widely used code for simulating groundwater flow in confined and unconfined aquifers, including pumping wells, recharge, evapotranspiration, drains and river–aquifer interaction (Harbaugh, 2005; Langevin et al., 2017). Its Newton formulation handles the drying and rewetting of unconfined cells that occur upstream of a barrier (Niswonger et al., 2011), and thin, low-permeability walls can be represented with the Horizontal Flow Barrier (HFB) package without refining the grid to the thickness of the wall (Hsieh & Freckleton, 1993). Senthilkumar and Elango (2011) used this approach to show that a subsurface barrier in southern India could raise upstream water levels and limit outflow, and the Japanese projects relied on comparable storage simulations to size their dams (Imaizumi, 2024). Modeling studies, however, seldom start from a systematic site screening, and they rarely evaluate the downstream consequences of storage in an aquifer that is already in deficit, where water retained upstream may simply be water removed from users downstream (Zhou, 2009).

The central question of this study is whether the technical, geological and hydrogeological conditions of the Rafsanjan Plain aquifer are suitable for constructing environmentally sustainable subsurface dams. To answer it, the study (i) defines the technical, hydrogeological, hydrological and environmental criteria that control subsurface-dam feasibility and uses them to screen the alluvial margins of the plain; (ii) develops, calibrates and validates a transient MODFLOW model of the aquifer; (iii) simulates cut-off walls at the highest-ranked sites under alternative design and climate scenarios; and (iv) evaluates the feasibility of each site by combining technical, hydrogeological and environmental indicators. The novelty of the work lies in assessing subsurface-dam feasibility with a calibrated numerical model rather than with descriptive criteria alone, and in weighing local storage gains against downstream outflow losses within the water budget of a severely depleted aquifer.

MATERIALS AND METHODS

Subsurface dams and their role in water-resources management

A subsurface dam is constructed to interrupt, reduce or control the natural groundwater flow in an alluvial aquifer and thereby increase the volume of water stored in the pore spaces of the subsurface materials. Two main types are usually distinguished: storage dams, which raise the water table behind an impermeable cut-off wall keyed into bedrock, and sand-storage dams, which trap coarse sediment and water in ephemeral channels (Lasage et al., 2008; Nilsson, 1988). Unlike surface dams, which store water in open reservoirs, subsurface dams retain water below ground level, so evaporation, surface contamination, health risks and the visual and social effects of reservoirs are much smaller (Ishida et al., 2011; Nilsson, 1988). Experience in different countries shows that subsurface dams can be used for local water supply, aquifer recharge, prevention of groundwater outflow, mitigation of drought impacts and support of sustainable agriculture (Hanson & Nilsson, 1986; Imaizumi, 2024). In arid regions, rivers are mostly seasonal and ephemeral, and surface flow occurs only during short rainfall periods. Storing the subsurface part of this flow helps to maintain access to water during dry periods, and because the water is protected from direct evaporation, subsurface storage can be more efficient than surface storage (Hanson & Nilsson, 1986; Nilsson, 1988).

Technical and hydrogeological criteria for subsurface dams

Feasibility assessment of a subsurface dam re-

quires the examination of geological, geotechnical, hydrological, hydrogeological and economic criteria. The main technical criteria are alluvial thickness, bedrock depth, the permeability and porosity of the materials, the presence of an impermeable layer at the base and abutments, the width of the valley or watercourse, the potential storage capacity of the alluvial reservoir, the availability of construction materials and the construction cost (Nilsson, 1988). If a site is unsuitable with respect to these criteria, construction may lead to low efficiency, high costs, leakage or structural instability. In practice, the depth at which a reliable cut-off can be built is a decisive constraint; in Japan, for example, grouting became very difficult at depths greater than about 50 m (Imaizumi, 2024). From a hydrogeological perspective, a site must have sufficient subsurface flow, adequate storage capacity in the alluvium, an appropriate balance between aquifer recharge and discharge, acceptable water quality and the ability to recover the stored water. Proper site selection is the most important stage in the success of a subsurface dam, because siting errors affect the performance of the entire project (Imaizumi, 2024; Ishida et al., 2011). Combined approaches that integrate field studies, geological data, geophysics, GIS and numerical modeling therefore improve the accuracy of decision-making (A. A. Jamali et al., 2018; Senthilkumar & Elango, 2011).

Case study: The Rafsanjan Plain aquifer

The Rafsanjan Plain lies in Kerman Province, southeastern Iran, within the Daranjir–Saghand basin. The plain covers about 12,500 km2, of which about 4,236 km2 is underlain by the alluvial aquifer, and it comprises the Rafsanjan, Noogh and Anar sub-plains. The climate is arid, with a mean annual rainfall of about 100 mm, falling mostly in winter and early spring, and a potential evapotranspiration of more than 3,000 mm. Surface runoff is restricted to ephemeral drainages that enter the plain from the surrounding highlands after storms, so groundwater is practically the only reliable source of water for domestic, agricultural and industrial use. The aquifer is mainly unconfined and consists of Quaternary alluvial deposits of sand, gravel, silt and clay overlying calcareous bedrock that acts as an impermeable base. The saturated thickness reaches about 100 m in the southwestern and central parts of the plain and decreases towards the northwest, while the depth to the water table ranges from about 5 m to more than 170 m. Coarse, highly permeable sediments dominate the southern, southwestern and southeastern margins, whereas finer and less permeable deposits prevail in the north and northwest. Groundwater flows generally from the southeast towards the northwest, and recharge occurs mainly along the northeastern and southeastern mountain fronts. Groundwater salinity increases along the flow path, and the northwestern part of the plain, where evaporite-bearing formations are present, has the poorest water quality. Pistachio cultivation dominates land use, and irrigation accounts for about 94% of groundwater withdrawals. Annual abstraction peaked at about 718 million m3 in 2007 and was about 667 million m3 in 2020, supplied by more than 1,400 authorised wells. Estimates of the annual groundwater deficit range from about 150 to 300 million m3. As a result, groundwater levels have declined almost continuously for about six decades, with drawdowns of up to 35 m relative to pre-development conditions, and land subsidence has reached rates of more than 5 cm yr−1 over large areas and more than 30 cm yr−1 locally. Cumulative subsidence of as much as 1.8 m was recorded near Noogh between 2014 and 2022.These conditions make the Rafsanjan Plain both a demanding and an appropriate case for testing subsurface dams. The arid climate, the strong dependence on groundwater, the declining water table and the high vulnerability to drought create a clear need for low-evaporation storage. At the same time, the deep alluvium of the central plain, the deficit of the aquifer and the saline northwestern zone impose constraints that must be evaluated quantitatively before a subsurface dam can be recommended. (Fig. 1)

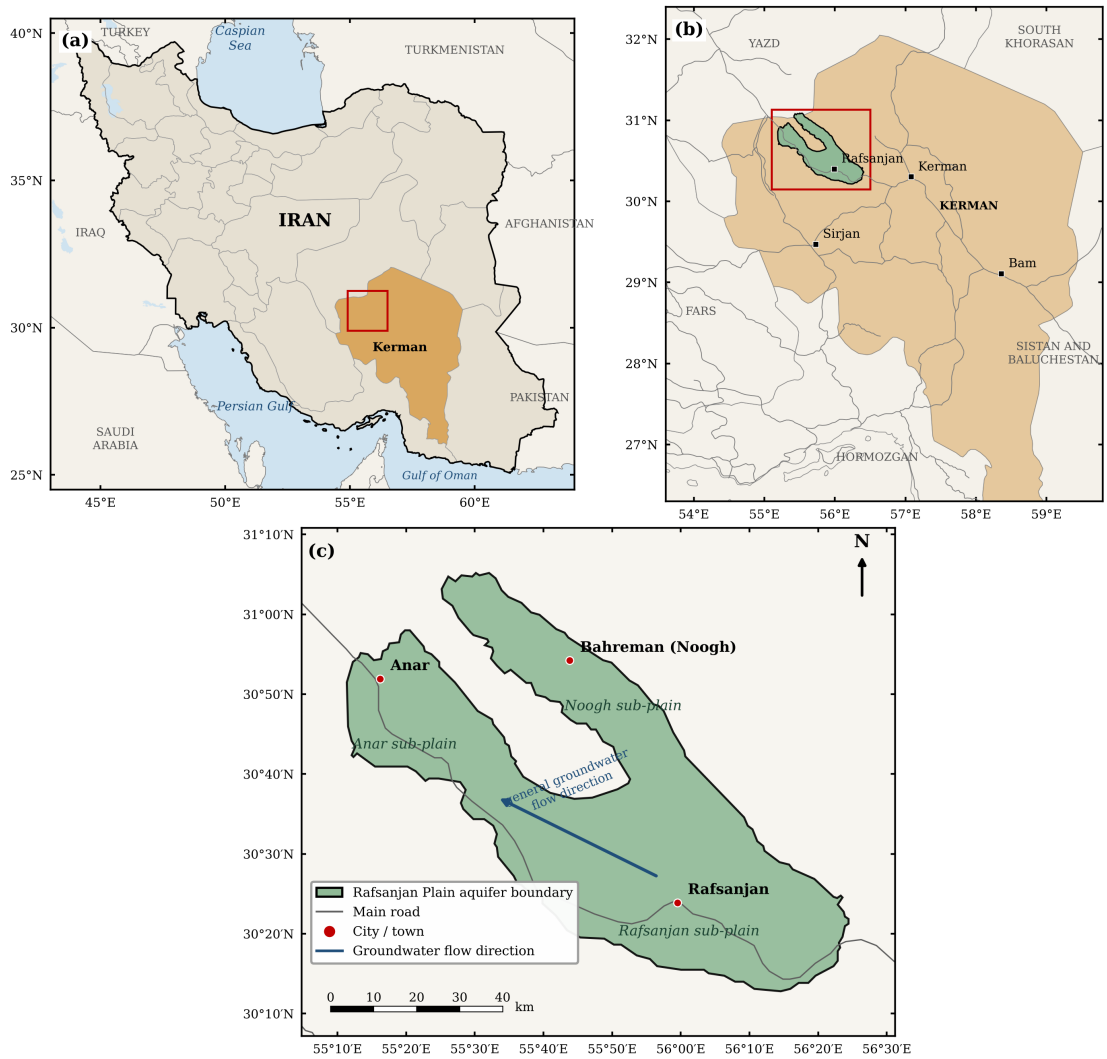


Figure 1: Location of the study area. (a) Position of Kerman Province in Iran; the red frame marks the Rafsanjan Plain. (b) The Rafsanjan Plain within Kerman Province, with the main towns and roads. (c) The Rafsanjan Plain aquifer and its three sub-plains (Anar, Noogh and Rafsanjan), showing the aquifer boundary, the main towns, the main road and the general direction of groundwater flow from southeast to northwest.

Research framework

The study is applied in purpose, because its results are intended to support decisions on groundwater-resource management, the selection of subsurface-dam sites and the mitigation of drought impacts in arid regions. In method, it is descriptive-analytical and is based on field studies, geological data, hydrological and hydrogeological information, geotechnical investigations and numerical modeling. The work followed a five-stage framework (Fig. 2): (1) data compilation; (2) definition of feasibility criteria and GIS-based screening of candidate sites; (3) development, calibration and validation of a transient groundwater-flow model; (4) simulation of cut-off walls at the highest-ranked sites under alternative scenarios; and (5) integrated assessment of technical, hydrogeological and environmental feasibility.

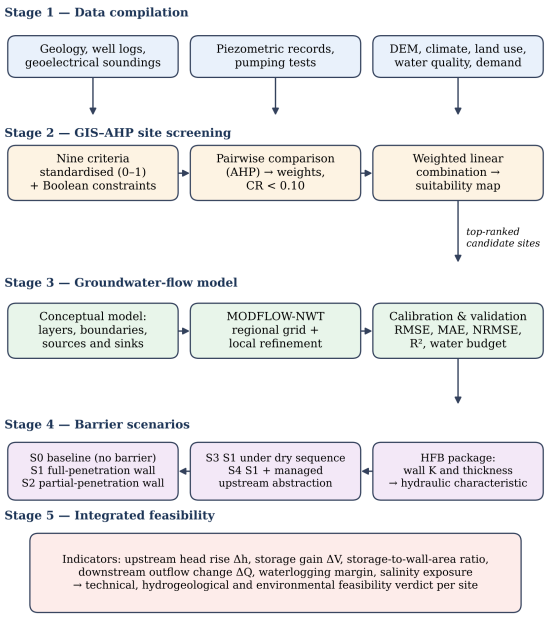


Figure 2: Methodological framework of the study.

Table 1 summarises the data used. They included regional geological and geomorphological information, topographic data, alluvial characteristics, bedrock conditions, rainfall and runoff records, production-well data, water-table levels, aquifer hydraulic parameters, geotechnical data and information on regional water demand. Lithological logs of exploration and production wells and geoelectrical soundings were used to map alluvial thickness and depth to bedrock. Water-level records from the observation-well network and pumping-test results provided heads and hydraulic parameters. For the numerical simulation, spatial and temporal groundwater-level data and aquifer boundary conditions were also used. (Tab .1)

Feasibility criteria and site screening

Screening was confined to the alluvial margins of the plain, where ephemeral drainages cross relatively thin alluvium before entering the main aquifer. This restriction reflects the basic engineering requirement that a cut-off wall be keyed into an impermeable base at a depth that can be reached with available construction methods (Imaizumi, 2024). Within this zone, nine criteria were selected on the basis of the subsurface-dam literature (Forzieri et al., 2008; Hanson & Nilsson, 1986; A. A. Jamali et al., 2018; I. A. Jamali et al., 2014; Nilsson, 1988) and grouped into four categories (Tab. 2). Geological and geotechnical criteria comprised the depth and type of bedrock (C1), the width of the alluvial cross-section at the dam axis, which controls wall length and abutment conditions (C2), and the distance from faults and evaporite-bearing formations, which affects sealing capability and water quality (C3). Hydrogeological criteria comprised saturated alluvial thickness (C4), hydraulic conductivity, which together with thickness determines transmissivity and subsurface flow (C5), and specific yield or effective porosity, which controls the ability of the alluvium to store water (C6). The hydrological criterion was the upstream catchment area, used as a proxy for runoff and natural recharge during wet and dry periods (C7). Environmental-sustainability criteria comprised groundwater salinity (C8) and the distance to points of demand, which reflects the advantages of local operation close to the point of use and the reduced need for a surface reservoir (C9). Built-up areas, protected areas and slopes steeper than 15% were excluded as Boolean constraints. Each criterion was converted to a raster with a cell size of 30 m and standardised to a 0–1 scale with linear functions bounded by the limits in (Tab. 2).

Criterion weights were derived with the Analytic Hierarchy Process (AHP) (Saaty, 2008). A panel of 12 experts in hydrogeology, geotechnical engineering and water-resources management compared the criteria pairwise on Saaty's 1–9 scale, and the individual judgements were aggregated with the geometric mean. The weight vector w was obtained as the principal eigenvector of the aggregated comparison matrix, and the consistency of the judgements was checked with the consistency index (CI) and consistency ratio (CR):

Table 1: Data used in the study.

Data	Source	Coverage / resolution	Use
Lithological logs and geoelectrical soundings	Kerman Regional Water Company	186 logs; 240 soundings	Bedrock depth, alluvial thickness, layering
Groundwater levels	Observation-well network	62 wells; monthly; 2001–2020	Initial heads, calibration, validation
Pumping tests	Kerman Regional Water Company	34 tests	K, T, Sy
Well inventory and abstraction	Kerman Regional Water Company	1,452 wells; 2020	Pumping (WEL), criterion C9
Rainfall and evaporation	IRIMO synoptic stations	daily; 1991–2020	Recharge, dry-sequence scenario
Digital elevation model	SRTM 1 arc-second	≈30 m	Slope, catchments, channels (C7)
Geological maps	Geological Survey of Iran	1:100,000	Bedrock, faults, evaporites (C1, C3)
Groundwater quality (EC)	Kerman Regional Water Company	58 samples; 2019	Criterion C8
Land use / land cover	Landsat 8 OLI classification	30 m; 2020	Constraints, demand points

Table 2: Criteria used for subsurface-dam site screening and their relationship with suitability.

Code	Criterion	Category	Effect on suitability	Standardisation limits
C1	Depth to impermeable bedrock	Geological–geotechnical	Decreases with depth	5–50 m
C2	Width of alluvial cross-section at axis	Geological–geotechnical	Decreases with width	50–1,500 m
C3	Distance from faults and evaporite formations	Geological–geotechnical	Increases with distance	0–5 km
C4	Saturated thickness	Hydrogeological	Increases with thickness	5–60 m
C5	Hydraulic conductivity	Hydrogeological	Increases with K	1–50 m d−1
C6	Specific yield	Hydrogeological	Increases with Sy	0.03–0.25
C7	Upstream catchment area	Hydrological	Increases with area	10–500 km2
C8	Groundwater salinity (EC)	Socio-environmental	Decreases with EC	1–10 dS m−1
C9	Distance to demand points	Socio-environmental	Decreases with distance	0–15 km

$$CI=(\lambda_max-n)/(n-1), \quad CR=CI/RI \qquad (1)$$

where λmax is the principal eigenvalue of the comparison matrix, n is the number of criteria and RI is the random index (1.45 for n = 9). Judgements were accepted when CR < 0.10 (Saaty, 2008). The suitability index (SI) of each cell was computed by weighted linear combination (Malczewski, 2006):

$$SI = \sum_{i=1}^{n} w_i x_i \cdot \prod_{j=1}^{m} c_j \qquad (2)$$

where xi is the standardised value of criterion i and cj is the Boolean value (0 or 1) of constraint j. The SI map was divided into five classes (very low to very high) with the natural-breaks method, and contiguous very-high-suitability cells that crossed an ephemeral channel were delineated as candidate dam axes. The three highest-ranked candidates (sites A, B and C) were carried forward to numerical modeling.

Numerical groundwater modeling

Governing equations

Groundwater flow was simulated with MODFLOW, which solves the governing equation for three-dimensional, transient flow in a hetero-

geneous and anisotropic porous medium by the finite-difference method (Harbaugh, 2005):

$$\frac{\partial}{\partial x}\left(K_{xx}\frac{\partial h}{\partial x}\right)+\frac{\partial}{\partial y}\left(K_{yy}\frac{\partial h}{\partial y}\right)+\frac{\partial}{\partial z}\left(K_{zz}\frac{\partial h}{\partial z}\right)+W=S_s\frac{\partial h}{\partial t} \quad (3)$$

where Kxx, Kyy and Kzz are the hydraulic conductivities in the x, y and z directions ($L\ T^{-1}$), h is hydraulic head (L), W is the volumetric recharge or abstraction term per unit volume (T^{-1}), Ss is specific storage (L^{-1}) and t is time. In unconfined layers, storage changes at the water table are governed by the specific yield Sy. This equation forms the basis for simulating changes in groundwater levels, flow direction and the effects of abstraction, recharge and subsurface barriers. Subsurface flow through the alluvium was estimated with Darcy's law:

$$Q=K\cdot i\cdot A \quad (4)$$

where Q is subsurface discharge ($L^3\ T^{-1}$), K is hydraulic conductivity, i is the hydraulic gradient and A is the cross-sectional area of flow (L^2). The hydraulic gradient between two points is

$$i=\Delta h/L \quad (5)$$

where Δh is the head difference and L the distance between the points. This relationship was used to analyse the direction and intensity of groundwater flow in the aquifer and across each proposed dam axis. The capacity of the aquifer to transmit water was expressed by the transmissivity

$$T=K\cdot b \quad (6)$$

where b is saturated thickness. The gross storage capacity of a subsurface reservoir depends on the volume of alluvium available for storage and on its effective porosity:

$$V=A\cdot H\cdot n_e \quad (7)$$

where V is the volume of water that can be stored, A is the effective area of the subsurface reservoir, H is the effective saturated thickness of the alluvium and ne is the effective porosity. Greater effective porosity and alluvial thickness therefore increase the storage capacity of a subsurface dam.

Conceptual model and discretisation

A conceptual model of the aquifer was developed from the geological structure, hydraulic boundaries, recharge and discharge conditions, locations of production wells and the hydraulic characteristics of the alluvium. The aquifer was represented by two layers above the impermeable calcareous base. Lateral inflow from the mountain fronts was simulated as a specified flux or with general-head boundaries, outflow at the northwestern margin with general-head boundaries, and the contact with outcropping bedrock elsewhere as a no-flow boundary. Recharge comprised infiltration of rainfall, infiltration from ephemeral channels during flow events and return flow from irrigation. Pumping was assigned by layer according to well-screen depth. Evapotranspiration from groundwater was neglected except where the water table is shallower than the extinction depth of 5 m. The model domain was discretised with a regional grid of 500 m × 500 m cells, refined to 50 m around the candidate sites so that the cut-off walls and the upstream reservoirs were resolved adequately. Input data included initial heads, hydraulic coefficients, recharge, abstraction and boundary conditions. MODFLOW-NWT was used because its Newton formulation remains stable when unconfined cells dry and rewet, as occurs upstream of a barrier during filling and drawdown cycles (Niswonger et al., 2011). The transient simulation covered water years 2001–2020 with monthly stress periods and was preceded by a steady-state simulation for 2000 that provided the initial heads.

Representation of the cut-off wall

Each cut-off wall was represented with the HFB package (Hsieh & Freckleton, 1993), which reduces the conductance between two adjacent cells according to the hydraulic characteristic of the barrier:

$$c_w=K_w/b_w \quad (8)$$

where Kw and bw are the hydraulic conductivi-

ty and thickness of the wall. The flow across the barrier between cells i and j is

$$Q_{ij} = C_{ij}(h_i - h_j) \quad C_{ij} = \left(\frac{1}{C_{ij}^0} + \frac{1}{c_w L_{ij} m_{ij}}\right)^{-1} \tag{9}$$

where Cij is the effective conductance of the connection between cells i and j, C0ij is the inter-cell conductance without the barrier, Lij is the length of the shared cell face and mij is the saturated thickness at the face (Fig.3). The wall was assigned the properties of a soil–cement or clay–cement diaphragm walls, with Kw = 1 × 10−8 m s−1 and bw = 0.6 m, consistent with the low-permeability walls used in practice (Imaizumi, 2024; Ishida et al., 2011). The hydraulic characteristic was varied by one order of magnitude in each direction in a sensitivity run to account for construction defects.

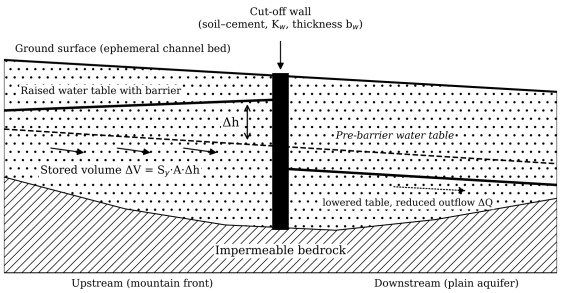


Figure 3: Schematic longitudinal section of a storage-type subsurface dam keyed into bedrock, showing the rise of the upstream water table (Δh), the stored volume (ΔV) and the reduced downstream outflow (ΔQ).

Calibration, validation and error indices

After the initial run, the model was calibrated to reduce the differences between observed and calculated groundwater levels. The steady-state model was calibrated first by adjusting hydraulic conductivity and recharge, after which the transient model was calibrated for 2001–2014 by adjusting specific yield, specific storage and the temporal distribution of recharge. Calibration combined trial-and-error adjustment with automated parameter estimation following the principles of Hill and Tiedeman (2007). The model was then validated, without further adjustment, against heads observed in 2015–2020. Model accuracy was evaluated with the root mean square error (RMSE), mean absolute error (MAE), RMSE normalised by the range of observed heads (NRMSE), mean error (ME) and coefficient of determination (R2) (Anderson et al., 2015):

$$RMSE = \sqrt{\frac{1}{N}\sum_{k=1}^{N}(h_{obsk} - h_{simk})^2} \tag{10}$$

$$MAE = \frac{1}{N}\sum_{k=1}^{N}|h_{obsk} - h_{simk}| \tag{11}$$

$$NRMSE = \frac{RMSE}{h_{obsmax} - h_{obsmin}} \times 100 \tag{12}$$

$$ME = \frac{1}{N}\sum_{k=1}^{N}(h_{simk} - h_{obsk}) \tag{13}$$

where $h_{obs,k}$ and $h_{sim,k}$ are the observed and simulated groundwater levels at observation k and N is the number of observations. Smaller RMSE and MAE values indicate a more accurate reproduction of aquifer behaviour. NRMSE < 10% was adopted as the calibration target, and the cumulative water-budget discrepancy was required to be below 1% (Anderson et al., 2015; Reilly & Harbaugh, 2004).

Simulation scenarios and feasibility indicators

Five scenarios were simulated for each candidate site over a 20-year horizon (Tab. 3). S0 represents current conditions without a barrier. S1 includes a cut-off wall keyed into bedrock across the full saturated thickness, and S2 a partially penetrating wall that closes 70% of the saturated thickness, representing a lower-cost design. S3 repeats S1 under a dry sequence in which recharge is reduced by 30% relative to the calibration period. S4 adds upstream abstraction equal to the simulated storage gain in S1, so that the stored water is used rather than merely retained.

Table 3: Simulated scenarios.

Scenario	Cut-off wall	Penetration	Recharge	Upstream abstraction
S0	None	–	Calibration-period mean	Current
S1	Yes	Full (keyed into bedrock)	Calibration-period mean	Current

S2	Yes	Partial (70%)	Calibration-period mean	Current
S3	Yes	Full	Reduced by 30%	Current
S4	Yes	Full	Calibration-period mean	Current + ΔV of S1

The hydrogeological benefit of each barrier was quantified as the increase in groundwater storage upstream of the wall relative to S0:

$$\Delta V=\sum_{(k\in U)} S_{(y,k)}\, A_k\, \Delta h_k \quad (14)$$

where Δh_k is the head difference between the barrier scenario and S0 in cell k of area A_k upstream of the wall, and $S_{y,k}$ is the specific yield of that cell. Because a deeper or longer wall is costlier, the technical efficiency of each design was expressed as the ratio of storage gain to wall area:

$$\eta=\Delta V/(L_w\, D_w) \quad (15)$$

where Lw and Dw are the length and depth of the wall. Downstream effects were expressed as the relative change in subsurface outflow across a control section located 500 m downstream of the wall:

$$\Delta Q_{rel}=(Q_{(out,S)}-Q_{(out,S0)})/Q_{(out,S0)} \times 100 \quad (16)$$

Two further indicators were used to check environmental constraints: the minimum depth to the water table upstream of the wall, which should remain greater than 2 m to avoid waterlogging and evaporative salinisation, and the change in the volume of groundwater flowing towards the saline northwestern zone.

Data analysis and integrated feasibility assessment

Data were analysed at three levels. At the first level, geological, geotechnical and hydrogeological data were examined to determine whether the physical conditions at each candidate site were suitable for construction. At the second level, the numerical results were interpreted to analyse changes in groundwater levels, the pattern of aquifer decline and the response of the aquifer to each barrier. At the third level, the technical and numerical findings were compared with environmental-sustainability criteria to determine feasibility from technical, hydrogeological and management perspectives.

For each candidate site, the results were combined in a feasibility matrix. Technical feasibility was judged from depth to bedrock, wall dimensions and construction method; hydrogeological feasibility from ΔV, η and the response to the dry sequence (S3); and environmental feasibility from ΔQrel, the waterlogging margin and the effect on flows towards the saline zone. A site was considered feasible only if it satisfied all three dimensions. This conservative rule reflects the principle that a local storage gain is acceptable only when it does not simply transfer the deficit to downstream users (Zhou, 2009).

FINDINGS AND DISCUSSION

Criterion weights and candidate sites

The aggregated pairwise comparison matrix was consistent (λmax = 9.62, CI = 0.078, CR = 0.053 < 0.10). Depth to bedrock (C1) received the largest weight (0.218), followed by hydraulic conductivity (C5, 0.162) and saturated thickness (C4, 0.141), whereas distance to demand (C9) received the smallest weight (0.047) (Tab. 4). The geological–geotechnical and hydrogeological criteria together account for 81.8% of the total weight, which reflects the expert consensus that a subsurface dam is feasible only where the barrier can be anchored in an impermeable base at moderate depth.

Very-high- and high-suitability classes together cover 307 km2, or 16.6% of the screened zone (Tab. 5). These classes are concentrated along the southern and southeastern margins, where coarse alluvial fans with high hydraulic conductivity are underlain by bedrock at relatively

shallow depth and receive runoff from the adjacent highlands. Low- and very-low-suitability classes dominate the northern and northwestern margins, where fine-grained sediments, low specific yield and the proximity of evaporite-bearing formations limit both the storage potential and the quality of the stored water. Three candidate axes (sites A, B and C) were identified within the very-high-suitability class; their characteristics are listed in (Tab. 6).

Table 4: AHP weights of the screening criteria.

Criterion	Weight	Rank
C1 Depth to bedrock	0.218	1
C2 Cross-section width	0.097	5
C3 Distance from faults/evaporites	0.082	6
C4 Saturated thickness	0.141	3
C5 Hydraulic conductivity	0.162	2
C6 Specific yield	0.118	4
C7 Catchment area	0.071	7
C8 Salinity (EC)	0.064	8
C9 Distance to demand	0.047	9
λmax / CI / CR	9.62 / 0.078 / 0.053	–

Table 5: Area of each suitability class in the screened zone.

Suitability class	Area (km2)	Share (%)
Very high	96	5.2
High	211	11.4
Moderate	448	24.2
Low	562	30.4
Very low	533	28.8
Total	1,850	100

Table 6: Characteristics of the candidate dam sites.

Site	Depth to bedrock (m)	Wall length (m)	Saturated thickness (m)	K (m d−1)	Sy (–)	Sl (–)
A	18	420	14	22	0.14	0.86
B	41	610	33	17	0.12	0.81
C	24	350	11	9	0.09	0.78

Model calibration and validation

The calibrated model reproduced the observed groundwater levels closely (Tab. 7). For the calibration period, RMSE was 2.84 m, MAE 2.17 m, NRMSE 3.9% and R2 0.96; for the validation period the corresponding values were 3.31 m, 2.58 m, 4.6% and 0.94. NRMSE remained below the 10% target in both periods, and a mean error of −0.42 m indicates slight underestimation of heads. The cumulative water-budget discrepancy was 0.21%. Calibrated hydraulic conductivity ranged from 0.4 m d−1 in the fine-grained northwestern sediments to 38 m d^{-1} in the southeastern fans, and specific yield from 0.04 to 0.18, consistent with the textural pattern of the aquifer described in Section 3.

Table 7: Performance of the groundwater-flow model.

Metric	Calibration (2001–2014)	Validation (2015–2020)
Number of observations, N	868	372
RMSE (m)	2.84	3.31
MAE (m)	2.17	2.58
NRMSE (%)	3.9	4.6
ME (m)	−0.42	−0.61
R2 (–)	0.96	0.94

The simulated water budget for the calibration period (Tab. 8) shows that pumping (652 million m^3 yr^1) exceeded total inflow (377 million m^3 yr−1), producing an average storage depletion of 290 million m^3 yr^1. This value lies within the range of deficit estimates reported for the plain (Bockstiegel et al., 2024), which provides an independent check on the model. The simulated decline of groundwater levels was greatest in the central and southwestern parts of the plain, where abstraction is concentrated. (Tab. 8) Simulated mean annual water budget of the aquifer for the calibration period (million m^3 yr^1).

Table 8: Simulated mean annual water budget of the aquifer for the calibration period

Component	Inflow	Outflow
Recharge from rainfall	38	–
Infiltration from ephemeral channels	46	–
Irrigation return flow	152	–
Lateral inflow (mountain fronts)	141	–
Pumping	–	652
Lateral outflow (northwest)	–	12
Evapotranspiration	–	3
Release from storage (depletion)	290	–
Total	667	667
Budget discrepancy (%)	0.21	

Response of the aquifer to the cut-off walls

At all three sites, the full-penetration wall (S1) produced a marked rise of the water table upstream and a smaller decline downstream. At site A, the maximum head rise immediately upstream of the wall was 6.8 m and decreased to less than 0.5 m at a distance of 2,300 m upstream. The storage gain reached 0.52 million m^3 after 6 years and then stabilised as the upstream water table approached a new equilibrium. The corresponding storage efficiency was 68.8 m3 m^2 of wall (Tab. 9). The partially penetrating wall (S2) achieved 74% of the storage gain of S1 with 70% of its wall area, indicating that full penetration is not strictly necessary at this site. The barriers reduced subsurface outflow across the downstream control sections by 22% to 41% (Tab. 9). Under the dry sequence (S3), the storage gains at site A fell to 0.37 million m3, a reduction of 29% relative to S1, but the upstream water table remained 4.6 m above that of S0. When the stored water was abstracted upstream (S4), the head rise was largely consumed while downstream outflow remained 9% below S0, which demonstrates that the barrier redistributes rather than creates water unless it intercepts flow that would otherwise be lost to the saline zone or to evaporation. The minimum

depth to the water table upstream of the walls was 3.4 m, so no waterlogging risk was identified.

Table 9: Response of the aquifer to the cut-off walls at the end of the simulation period.

Site	Scenario	Max. Δh (m)	ΔV (10^6 m^3)	η (m3 m^{-2})	ΔQ_{rel} (%)	Min. depth to water table (m)
A	S1	6.8	0.52	68.8	−27	3.4
A	S2	5.0	0.38	72.7	−19	5.2
A	S3	4.6	0.37	48.9	−24	5.6
A	S4	1.3	0.09	11.9	−9	8.9
B	S1	5.1	0.71	28.4	−22	4.1
B	S2	3.6	0.50	28.6	−15	5.6
B	S3	3.4	0.49	19.6	−19	5.8
B	S4	1.0	0.12	4.8	−7	8.2
C	S1	4.2	0.21	25.0	−41	3.6
C	S2	3.0	0.15	25.5	−30	4.8
C	S3	2.7	0.14	16.7	−36	5.1
C	S4	0.8	0.04	4.8	−16	7.0

Integrated feasibility

The feasibility matrix (Tab. 10) shows that site A satisfied all technical, hydrogeological and environmental criteria and is therefore recommended as the preferred site. Site B was hydrogeologically favourable but technically constrained by a bedrock depth of 41 m, which would require a wall area of 25,010 m^2. Site C produced the smallest storage gain and the largest relative reduction of downstream outflow, and it was therefore classified as not feasible under the conservative rule adopted in Section 4.6.

Table 10: Integrated feasibility matrix of the candidate sites.

Site	Technical	Hydrogeological	Environmental	Overall
A	Feasible	Feasible	Feasible	Feasible – preferred
B	Constrained	Feasible	Feasible	Conditionally feasible
C	Feasible	Limited	Not feasible	Not feasible

RESULTS AND CONCLUSION

Technical controls on subsurface-dam feasibility

The results confirm that depth to bedrock is the decisive technical constraint on subsurface dams in large alluvial basins. Over most of the Rafsanjan Plain the alluvium is about 100 m thick (Hosseininia & Hassanzadeh, 2023), so a barrier across the main aquifer would be neither economical nor technically realistic. Opportunities exist only along the plain margins, where alluvial fans thin towards the mountain front. This agrees with the general guidance that groundwater dams are best suited to narrow valleys with shallow, impermeable bedrock (Hanson & Nilsson, 1986; Nilsson, 1988) and with the Japanese experience, in which feasibility was strongly site-specific and limited by the depth at which a reliable cut-off could be constructed (Imaizumi, 2024). It also explains why the AHP assigned the largest weight to C1 and why the suitable sites are spatially concentrated rather than spread across the plain

Hydrogeological controls on storage performance

Hydraulic conductivity and specific yield control the hydrogeological part of the trade-off. High conductivity allows the reservoir behind the wall to fill quickly after recharge events but also increases leakage through construction defects and around the ends of the wall, which is why the sensitivity runs on the hydraulic characteristic are important. Specific yield controls how much water a given head rise represents (Eqs. 7 and 14); the design value of about 10% adopted for the Japanese dams (Imaizumi, 2024) provides a useful benchmark for the calibrated values obtained here. Comparable head rises upstream of a modelled barrier were also reported by Senthilkumar and Elango (2011), which supports the use of the HFB approach for feasibility studies of this kind.

Local storage gains versus basin-scale water budget

The scenario results show that a subsurface dam in an over-drafted basin does not create new water; it changes where and when water is available. In a closed basin, water retained upstream would otherwise have flowed to downstream wells, so a local storage gain can simply reproduce the existing deficit elsewhere (Zhou, 2009). The net benefit of a barrier in the Rafsanjan Plain therefore depends on what the intercepted water would otherwise have done. Water that would have reached the fine-grained, saline northwestern part of the aquifer (Hosseininia & Hassanzadeh, 2023), or that would have been lost from shallow water tables to evaporation, represents a genuine gain in usable fresh water; water that would have reached productive downstream wells does not. The downstream outflow indicator (Eq. 16) and scenario S4 make this distinction explicit and should be part of any feasibility assessment of subsurface storage in depleted aquifers.

Environmental sustainability and implications for management

Subsurface dams have clear environmental advantages over surface reservoirs in this climate: evaporation from the stored water is negligible, no land is flooded, and the stored water is protected from contamination (Ishida et al., 2011; Nilsson, 1988). Locally higher water tables upstream of a barrier may also reduce further compaction of fine-grained layers, the mechanism behind the severe subsidence observed in the plain (Bockstiegel et al., 2024; Motagh et al., 2017). These benefits, however, are local. The basin-wide deficit of the Rafsanjan aquifer is driven by abstraction for irrigation (Bockstiegel et al., 2024; Madani, 2014), and no storage structure can offset a deficit of several hundred million cubic metres per year. Subsurface dams should therefore be regarded as a complement to demand management and to other forms of managed aquifer recharge (Dillon et al., 2019), best suited to supplying villages and orchards near the mountain front during dry periods. This study assessed the technical and hydrogeological feasibility of environmentally sustainable subsurface dams in the Rafsanjan Plain aquifer, one of the most severely over-exploited aquifers in arid Iran. Feasibility criteria derived from the subsurface-dam literature were used to screen the alluvial margins of the plain, and a transient MODFLOW model, calibrated and validated against observed groundwater levels, was used to simulate cut-off walls at the highest-ranked sites under five design and climate scenarios. By evaluating the hydraulic response of the aquifer explicitly, the study moves beyond the descriptive site-suitability assessments that dominate the literature and provides a quantitative basis for deciding whether, where and how subsurface dams should be built in a depleted basin.

Technical and Hydrogeological feasibility

Depth to impermeable bedrock was the most influential factor in the feasibility of subsurface dams, followed by hydraulic conductivity and saturated thickness, which together with bedrock depth received 52.1% of the total criterion weight. Because the alluvium of the central plain is about 100 m thick, a cut-off wall across the main aqui-

fer is not technically or economically realistic. Feasible sites are confined to the coarse alluvial fans of the southern and southeastern margins, where bedrock is relatively shallow, the alluvial cross-section is narrow and the wall can be keyed into an impermeable base. At the preferred site, a wall 420 m long and 18 m deep would be required, which is within the range of established construction methods such as soil–cement diaphragm walls. The storage-to-wall-area ratio of 68.8 m^3 m^{-2} proved a practical indicator for comparing designs and sites, and the partially penetrating design achieved 74% of the storage gain of the full-penetration design, showing that a lower-cost design may be acceptable.

Also, the calibrated model reproduced observed groundwater levels with an RMSE of 2.84 m, an MAE of 2.17 m and an NRMSE of 3.9%, and the simulated storage depletion of 290 million m3 yr−1 was consistent with independent deficit estimates for the plain. This confirms that the model represents the main features of aquifer behaviour and can be used to evaluate barrier scenarios. At the preferred site, a full-penetration wall raised upstream groundwater levels by up to 6.8 m and added 0.52 million m3 of recoverable storage, with the new equilibrium reached after about 6 years. Under a dry sequence, the storage gain decreased by 29% but remained positive, indicating that the subsurface reservoir can provide a buffer during droughts. The results also show that storage performance depends directly on effective porosity and saturated thickness, so accurate characterisation of these properties through drilling, geophysics and pumping tests is a prerequisite for reliable design. Subsurface dams store water with negligible evaporation, occupy little land and protect the stored water from contamination, which makes them an environmentally sustainable storage option for the arid climate of the Rafsanjan Plain. However, the barriers reduced downstream subsurface outflow by 22%–41%, demonstrating that in an over-drafted basin a subsurface dam redistributes water rather than creating it. A genuine gain in usable fresh water arises mainly where the intercepted flow would otherwise reach the saline northwestern zone or be lost to evaporation. The minimum depth to the water table upstream of the walls remained 3.4 m, so the dams would not cause waterlogging or evaporative salinisation. Locally higher groundwater levels may also slow the compaction of fine-grained layers and reduce subsidence near the dam sites.

REFERENCES

Anderson, M. P., Woessner, W. W., & Hunt, R. J. (2015). Applied groundwater modeling: Simulation of flow and advective transport (2nd ed.). Academic Press. https://pubs.usgs.gov/publication/70160331

Ashraf, S., Nazemi, A., & AghaKouchak, A. (2021). Anthropogenic drought dominates groundwater depletion in Iran. Scientific Reports, 11, Article 9135. https://doi.org/10.1038/s41598-021-88522-y

Bockstiegel, M., Richard-Cerda, J. C., Muñoz-Vega, E., Haghshenas Haghighi, M., Motagh, M., Lalehzari, R., & Schulz, S. (2024). Simulation of present and future land subsidence in the Rafsanjan plain, Iran, due to groundwater overexploitation using numerical modeling and InSAR data analysis. Hydrogeology Journal, 32(1), 289–305. https://doi.org/10.1007/s10040-023-02657-y

Dillon, P., Stuyfzand, P., Grischek, T., Lluria, M., Pyne, R. D. G., Jain, R. C., Bear, J., Schwarz, J., Wang, W., Fernandez, E., Stefan, C., Pettenati, M., van der Gun, J., Sprenger, C., Massmann, G., Scanlon, B. R., Xanke, J., Jokela, P., Zheng, Y., … Sapiano, M. (2019). Sixty years of global progress in managed aquifer recharge. Hydrogeology Journal, 27(1), 1–30. https://doi.org/10.1007/s10040-018-1841-z

Famiglietti, J. S. (2014). The global groundwater crisis. Nature Climate Change, 4(11), 945–948. https://doi.org/10.1038/nclimate2425

Forzieri, G., Gardenti, M., Caparrini, F., & Castelli, F. (2008). A methodology for the pre-selection of suitable sites for surface and underground small dams in arid areas: A case study in the region of Kidal, Mali. Physics and Chemistry of the Earth, Parts A/B/C, 33(1–2), 74–85. https://

doi.org/10.1016/j.pce.2007.04.014
Gleeson, T., Wada, Y., Bierkens, M. F. P., & van Beek, L. P. H. (2012). Water balance of global aquifers revealed by groundwater footprint. Nature, 488(7410), 197–200. https://doi.org/10.1038/nature11295
Gorelick, S. M., & Zheng, C. (2015). Global change and the groundwater management challenge. Water Resources Research, 51(5), 3031–3051. https://doi.org/10.1002/2014WR016825
Hanson, G., & Nilsson, Å. (1986). Ground-water dams for rural-water supplies in developing countries. Ground Water, 24(4), 497–506. https://doi.org/10.1111/j.1745-6584.1986.tb01029.x
Harbaugh, A. W. (2005). MODFLOW-2005, the U.S. Geological Survey modular ground-water model—The ground-water flow process (Techniques and Methods 6-A16). U.S. Geological Survey. https://doi.org/10.3133/tm6A16
Hill, M. C., & Tiedeman, C. R. (2007). Effective groundwater model calibration: With analysis of data, sensitivities, predictions, and uncertainty. John Wiley & Sons. https://doi.org/10.1002/0470041080
Hosseininia, M., & Hassanzadeh, R. (2023). Groundwater quality assessment for domestic and agricultural purposes using GIS, hydrochemical facies and water quality indices: Case study of Rafsanjan plain, Kerman province, Iran. Applied Water Science, 13, Article 84. https://doi.org/10.1007/s13201-023-01891-9
Hsieh, P. A., & Freckleton, J. R. (1993). Documentation of a computer program to simulate horizontal-flow barriers using the U.S. Geological Survey's modular three-dimensional finite-difference ground-water flow model (Open-File Report 92-477). U.S. Geological Survey. https://doi.org/10.3133/ofr92477
Imaizumi, M. (2024). Review of subsurface dam technology based on Japan's experience in the Ryukyu Arc. Water, 16(16), Article 2282. https://doi.org/10.3390/w16162282
Ishida, S., Tsuchihara, T., Yoshimoto, S., & Imaizumi, M. (2011). Sustainable use of groundwater with underground dams. Japan Agricultural Research Quarterly, 45(1), 51–61. https://doi.org/10.6090/jarq.45.51
Jamali, A. A., Randhir, T. O., & Nosrati, J. (2018). Site suitability analysis for subsurface dams using Boolean and fuzzy logic in arid watersheds. Journal of Water Resources Planning and Management, 144(8), Article 04018047. https://doi.org/10.1061/(ASCE)WR.1943-5452.0000947
Jamali, I. A., Mörtberg, U., Olofsson, B., & Shafique, M. (2014). A spatial multi-criteria analysis approach for locating suitable sites for construction of subsurface dams in Northern Pakistan. Water Resources Management, 28(14), 5157–5174. https://doi.org/10.1007/s11269-014-0800-2
Joodaki, G., Wahr, J., & Swenson, S. (2014). Estimating the human contribution to groundwater depletion in the Middle East, from GRACE data, land surface models, and well observations. Water Resources Research, 50(3), 2679–2692. https://doi.org/10.1002/2013WR014633
Konikow, L. F., & Kendy, E. (2005). Groundwater depletion: A global problem. Hydrogeology Journal, 13(1), 317–320. https://doi.org/10.1007/s10040-004-0411-8
Langevin, C. D., Hughes, J. D., Banta, E. R., Niswonger, R. G., Panday, S., & Provost, A. M. (2017). Documentation for the MODFLOW 6 groundwater flow model (Techniques and Methods 6-A55). U.S. Geological Survey. https://doi.org/10.3133/tm6A55
Lasage, R., Aerts, J., Mutiso, G.-C. M., & de Vries, A. (2008). Potential for community based adaptation to droughts: Sand dams in Kitui, Kenya. Physics and Chemistry of the Earth, Parts A/B/C, 33(1–2), 67–73. https://doi.org/10.1016/j.pce.2007.04.009
Madani, K. (2014). Water management in Iran: What is causing the looming crisis? Journal of Environmental Studies and Sciences, 4(4), 315–328. https://doi.org/10.1007/s13412-014-0182-z
Malczewski, J. (2006). GIS-based multicriteria decision analysis: A survey of the literature. International Journal of Geographical Information Science, 20(7), 703–726. https://doi.org/10.1080/13658810600661508
Motagh, M., Walter, T. R., Sharifi, M. A., Fielding, E., Schenk, A., Anderssohn, J., & Zschau, J. (2008). Land subsidence in Iran caused by widespread water reservoir overexploitation. Geophysical Research Letters, 35(16), Article L16403.

https://doi.org/10.1029/2008GL033814

Motagh, M., Shamshiri, R., Haghshenas Haghighi, M., Wetzel, H.-U., Akbari, B., Nahavandchi, H., Roessner, S., & Arabi, S. (2017). Quantifying groundwater exploitation induced subsidence in the Rafsanjan plain, southeastern Iran, using InSAR time-series and in situ measurements. Engineering Geology, 218, 134–151. https://doi.org/10.1016/j.enggeo.2017.01.011

Nilsson, Å. (1988). Groundwater dams for small-scale water supply. Intermediate Technology Publications. https://doi.org/10.3362/9781780442297

Niswonger, R. G., Panday, S., & Ibaraki, M. (2011). MODFLOW-NWT, a Newton formulation for MODFLOW-2005 (Techniques and Methods 6-A37). U.S. Geological Survey. https://doi.org/10.3133/tm6A37

Noori, R., Maghrebi, M., Mirchi, A., Tang, Q., Bhattarai, R., Sadegh, M., Noury, M., Torabi Haghighi, A., Kløve, B., & Madani, K. (2021). Anthropogenic depletion of Iran's aquifers. Proceedings of the National Academy of Sciences, 118(25), Article e2024221118. https://doi.org/10.1073/pnas.2024221118

Reilly, T. E., & Harbaugh, A. W. (2004). Guidelines for evaluating ground-water flow models (Scientific Investigations Report 2004-5038). U.S. Geological Survey. https://doi.org/10.3133/sir20045038

Saaty, T. L. (2008). Decision making with the analytic hierarchy process. International Journal of Services Sciences, 1(1), 83–98. https://doi.org/10.1504/IJSSCI.2008.017590

Senthilkumar, M., & Elango, L. (2011). Modelling the impact of a subsurface barrier on groundwater flow in the lower Palar River basin, southern India. Hydrogeology Journal, 19(4), 917–928. https://doi.org/10.1007/s10040-011-0735-0

Wada, Y., van Beek, L. P. H., van Kempen, C. M., Reckman, J. W. T. M., Vasak, S., & Bierkens, M. F. P. (2010). Global depletion of groundwater resources. Geophysical Research Letters, 37(20), Article L20402. https://doi.org/10.1029/2010GL044571

Zhou, Y. (2009). A critical review of groundwater budget myth, safe yield and sustainability. Journal of Hydrology, 370(1–4), 207–213. https://doi.org/10.1016/j.jhydrol.2009.03.009

COPYRIGHTS

©2023 The author(s). This is an open access article distributed under the terms of the Creative Commons Attribution (CC BY 4.0), which permits unrestricted use, distribution, and reproduction in any medium, as long as the original authors and source are cited. No permission is required from the authors or the publishers.

HOW TO CITE THIS ARTICLE

Riahi Riseh, S., Robati, A. & Kazerooni Sadi, M. (2026). Numerical and Empirical Assessment of Wave Transmission over Submerged Dams: A Comparison of the SWAN Spectral (Grid) Model with Empirical Formulae for Low-Crested Structures. (e743126). International Journal of Urban Management and Energy Sustainability, ( ), e743126

DOI:10.22034/ijumes.2026.2108047.1418